

## Phase transformation and densification of nanostructured alumina. Effect of seeding and doping

C. Legros<sup>1,a</sup>, C. Carry<sup>2,b</sup>, S. Lartigue-Korinek<sup>3,c</sup>, P. Bowen<sup>4,d</sup>

<sup>1</sup>Laboratoire d'Etude des Matériaux Hors Equilibre, CNRS UMR 8647, Université Paris XI,  
F-91405 Orsay Cedex, France

<sup>2</sup>Laboratoire de Thermodynamique et Physico-Chimie Métallurgique, CNRS UMR 5614,  
INPG/UJF, F-38402 Saint Martin d'Hères Cedex, France

<sup>3</sup>Centre d'Etudes de Chimie Métallurgique, CNRS UPR 2801, 15 rue Georges Urbain,  
F-94407 Vitry-sur-Seine, France

<sup>4</sup>Laboratoire de Technologie des Poudres, DMX, EPFL, CH-1015 Lausanne, Switzerland

<sup>a</sup>[corinne.legros@lemhe.u-psud.fr](mailto:corinne.legros@lemhe.u-psud.fr)

<sup>b</sup>[claudio.carry@ltpcm.inpg.fr](mailto:claudio.carry@ltpcm.inpg.fr)

<sup>c</sup>[sylvie.lartigue@glvt-cnrs.fr](mailto:sylvie.lartigue@glvt-cnrs.fr)

<sup>d</sup>[paul.bowen@epfl.ch](mailto:paul.bowen@epfl.ch)

**Keywords:**  $\gamma$  nanocrystalline alumina, diffusive phase transformation, sintering, coarsening, grain growth, seeding, doping, segregation, precipitation.

**Abstract.** By following the densification kinetics of nanocrystalline  $\gamma$  alumina and corresponding microstructural evolution we showed that the diffusive transformation gamma-alpha involves several processes such as nucleation of alpha phase, rearrangement of gamma crystallite at alpha seed and grain surfaces, formation of porous alpha alumina monocrystalline colonies. Results concerning the effects of seeding and doping elements on the transformation-densification behaviour of the same  $\gamma$ -alumina raw powder batch are also presented. Doping elements seem to have no influence on nucleation rate but could modify the redistribution rate of the ions during the transformation by short range diffusion of doping elements.

### Introduction

Nanocrystalline aluminas could be of interest for technological applications in electronic and mechanical properties. Most nanostructured oxide powders are metastable and undergo phase transformations during sintering. Dense nanocrystalline ceramics such as  $\text{TiO}_2$  or  $\text{ZrO}_2$  have been obtained [1-2]. For alumina, the phase transformation generally results in development of vermicular microstructures. The final stages of sintering then require very high temperatures to achieve high densities [3]. Improvement may be obtained by  $\alpha$ - $\text{Al}_2\text{O}_3$  seeding of the initial precursors gels or powders [4-5], pressure sintering methods [6], doping of gamma powders with different elements [7-8] or colloidal processing methods [9-10].

However, in general no paper has reported an enhancement or retardation of the  $\gamma$  to  $\alpha$  phase transformation of a sufficient magnitude to lead to high-density nanograined centimetric material parts at sintering temperatures lower than those used for fine grained  $\alpha$ - $\text{Al}_2\text{O}_3$  powders. In this context, a better understanding of this phase transformation is needed for producing dense nanocrystalline alumina.

The aim of this work is to follow the densification kinetics of nanocrystalline  $\gamma$  alumina and corresponding microstructural evolution to hope to elucidate the key mechanism of such diffusive

phase transformation assisted densification; our ultimate goal being to prepare  $\alpha$ -Al<sub>2</sub>O<sub>3</sub> nanoceramics starting from undoped or doped nanocrystalline  $\gamma$ -Al<sub>2</sub>O<sub>3</sub>, without pressure assisted sintering.

## Powders and Experimental Procedures

The two undoped batches used in this work were provided by Baikowski Chimie (France) and correspond to the Baikalox CR125 commercial grade which is an alum derived  $\gamma$ -alumina with a specific area of 100 m<sup>2</sup>/g. They differ mainly from one another in initial  $\alpha$ -alumina content: the batch 0 $\alpha$  has an  $\alpha$  initial content less than 0.5% although the batch 6 $\alpha$  is seeded with 6%  $\alpha$ -phase.

M-doped samples (cationic ratio M/Al ranging from 0 to 9600 ppm) were prepared from a slurry in propane-2-ol of the batch 0 $\alpha$ . For a given doping level, the corresponding amount of an aqueous nitrate solution (Mg, Y, Zr) or titanium isopropoxyde solution was poured into the alumina slurry. Then, each slurry was dried and later calcined in an oxygen flow at 670°C or 800°C for 24h. This procedure is expected to yield a uniform repartition of the dopant in alumina particles and does not modify the  $\alpha$  initial content. Various doped samples are labelled by their cationic ratio (ppm/100), for example 32Ti means a doping of 3194 ppm Ti/Al or 0.5 wt %TiO<sub>2</sub>.

The sintering behaviours are studied by dilatometry (TMA92 Setaram, France) in air. Densities,  $\rho(T)$ , and densification rate curves were computed from the recorded shrinkage data and from the final densities measured by the classical Archimede's method on cooled samples. The densification tests are interrupted at different stages of the heat treatment prior their analysis by Transmission Electron Microscopy (TEM) or pore size measurements. Conventional TEM experiments are performed on a JEOL 2000EX operating at 200kV. Thin foils are prepared by classical methods of mechanical polishing and ion milling at 5kV. The nanometric pore sizes were measured from hysteresis of adsorption and desorption nitrogen isotherms (B.E.T. method).

## Results and discussion

Figure 1 illustrates the effect of various parameters on densification under constant heating rate (1 or 10°C/min) up to 1450 or 1550°C. Dilatometry curves for all samples show two regimes: the first R1 is a densification associated with the phase transformation of  $\gamma$ -Al<sub>2</sub>O<sub>3</sub> to  $\alpha$ -Al<sub>2</sub>O<sub>3</sub> at around 1100°C, the second R2 is the densification of the  $\alpha$ -phase at higher temperatures.

The temperature of first densification rate peak, R1, is significantly influenced by heating rate and seeding with  $\alpha$ -particles; both factors lowering R1.

The transformation relative density variation,  $\Delta\rho_R$  (Fig. 1), is much higher than the increase of density from  $\gamma$  to  $\alpha$  (10.75% with 3.6 g.cm<sup>-3</sup> for  $\gamma$ -phase). Significant differences in  $\Delta\rho_R$  values are observed and depend on powder batch and heating rate.

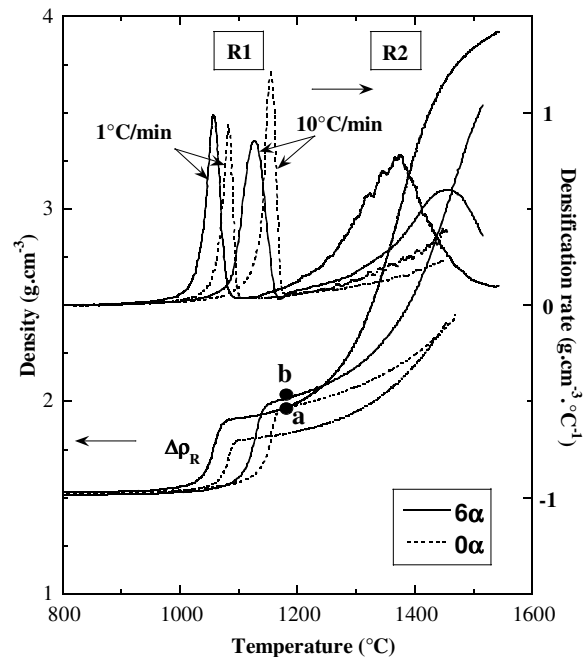


Fig. 1: densification curves of  $\gamma$  alumina compacts (250MPa CIP) unseeded or seeded with 6%  $\alpha$ -alumina for two heating rates.

The porosity of samples from interrupted dilatometric runs during the first densification regime R1 (up to 1180°C) was investigated using nitrogen porosimetry. Figure 2 shows the evolution of nanopore volume fraction and  $\alpha$ -phase content (determined from neutron diffraction diagram) for two different heating rates. It seems that when the transformation from  $\gamma$  to  $\alpha$  phase takes place, all the nanopore volume fraction is eliminated, excepted for the batch 6 $\alpha$  sample heated at 10°C/min. These results are in good agreement with previous determinations only done at 1180°C [5].

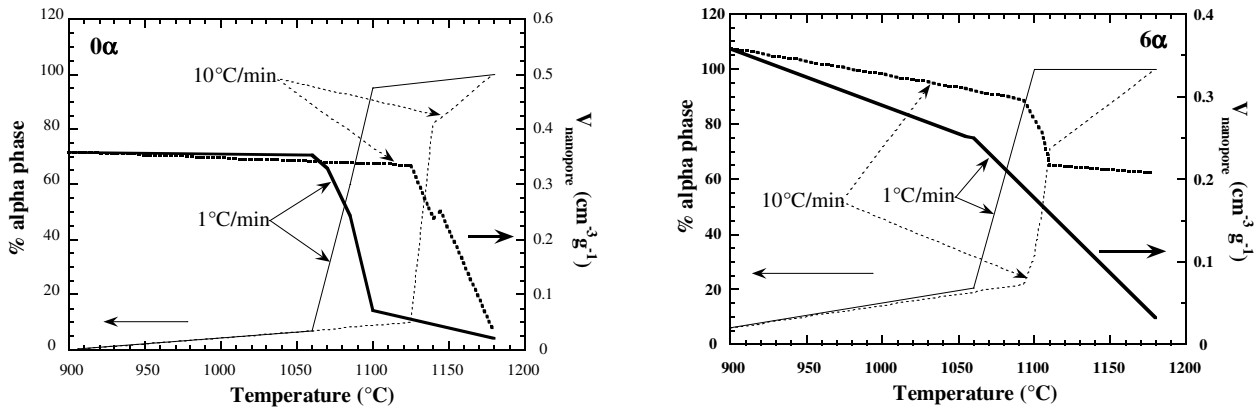


Fig. 2: evolution of  $\alpha$ -phase content and nanopore volume (BET) during the first densification regime R1 (up to 1180°C) for two different heating rates.

After the phase transformation, the microstructure of the porous alumina is a mosaic of clusters called colonies assembling nanosized grains with similar orientations (Fig.3), these colonies can be considered as porous monocrystalline zone. It seems that the final size of the colonies at the end of the transformation is correlated to the number of  $\alpha$ -alumina seeds in the starting  $\gamma$ -alumina powder.

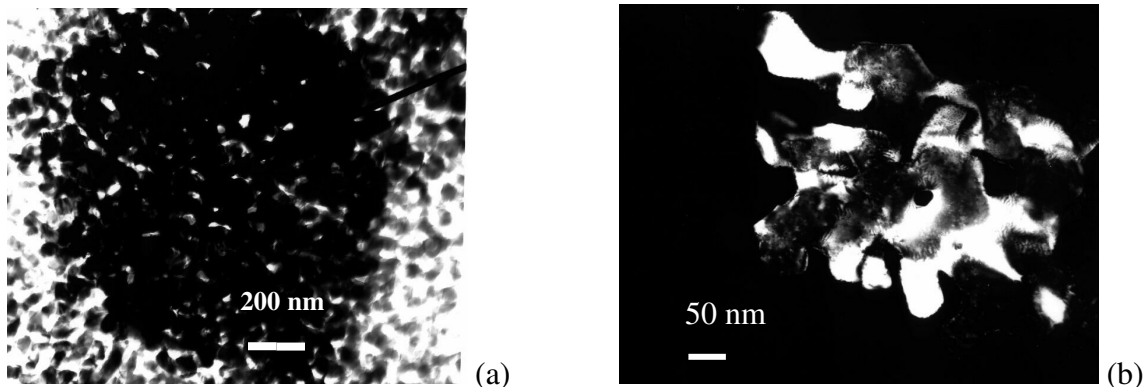


Fig. 3: TEM bright field image of (a) 0 $\alpha$  sample (interrupted test a, Fig. 1) and (b) 6 $\alpha$  sample (interrupted test b, Fig. 1) at 1180°C showing porous monocrystalline colonies composed of elementary bricks with similar orientations.

The formation of stable phase from metastable transition phase occurs by a nucleation and controlled diffusion grain growth process during heating. But the above observations suggest that a grain rearrangement process is coupled with the phase transformation. Coupled mechanisms of transformation, rearrangement and coarsening from nucleation sites lead to the formation of monocrystalline porous colonies (Fig. 4). In fact, when a particle transforms from  $\gamma$  to  $\alpha$  phase, if the neighboring grains are not close packed or not symmetrically arranged, the crystallographic volume reduction can induce non-symmetrical inter-particle forces causing particles or grains to slide and to rotate. Such relative particle movement leads to particle rearrangement, the amplitude of which depends on the free space available (porosity) and on the density of nucleation sites. These

mechanisms of rearrangement and microstructural homogenization illustrated in this work on transition aluminas should also be applicable to other nanometric oxide powders which are often metastable and incur a phase transformation during sintering, see for example reference 11.

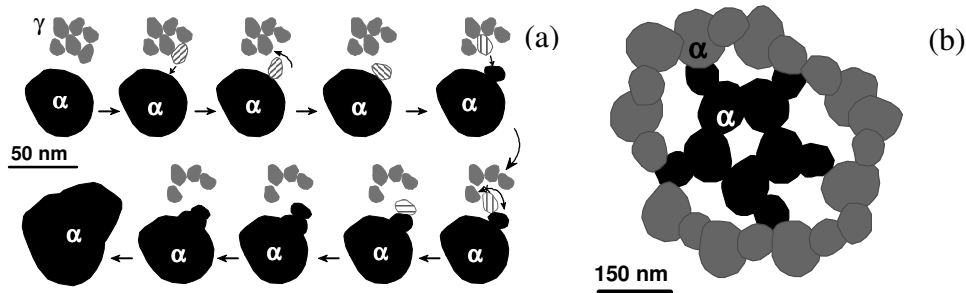


Fig. 4: a) schematic coupled mechanisms of particle rearrangement and coalescence during  $\gamma$ - $\alpha$  phase transformation, b)  $\alpha$  growing porous monocrystalline colonies composed of elementary bricks.

After transformation, densification arises first from intra-colonies densification by a decrease of internal porosity due to coarsening of elementary bricks of porous colonies. The lower the intra-colonie pore volume fraction is, the fastest the densification rate of the monocrystalline colonies is because at this temperature, the coarsening of bricks depends mainly on surface diffusion. This step of densification is rapid when materials are composed of smallest bricks and more dense colonies. Thereafter, a classical sintering process of dense colonies promotes the suppression of intergranular porosity. Consequently, the second densification rate peak R2 occurs at a more lowest temperature. Unfortunately, at the end of the sintering, the microstructure is always composed of micrometric grains.

Figure 5 exhibits the effect of doping on densification behaviour of unseeded transition alumina compacts sintered at constant heating rate ( $1^\circ/\text{min}$ ) up to  $1550^\circ\text{C}$ . The two classical regimes (R1 and R2) of densification of such  $\gamma$ -alumina compacts are observed. Y and Zr shift the transformation to higher temperatures and Mg and Ti have a much less pronounced effect. Doping seems to have no influence on nucleation rate as evidenced the same temperature of beginning of the phase transformation, whatever the doping nature. But we can suppose that it could modify the redistribution rate of the ions during the transformation by short range diffusion of doping elements. In a doped  $\alpha$ -alumina, the doping element may be distributed : as a lattice solid solute, as a grain boundary (GB) segregant beyond saturation of the lattice solid solution, and as a second phase precipitate upon saturation of both the GB and the lattice solid solution.

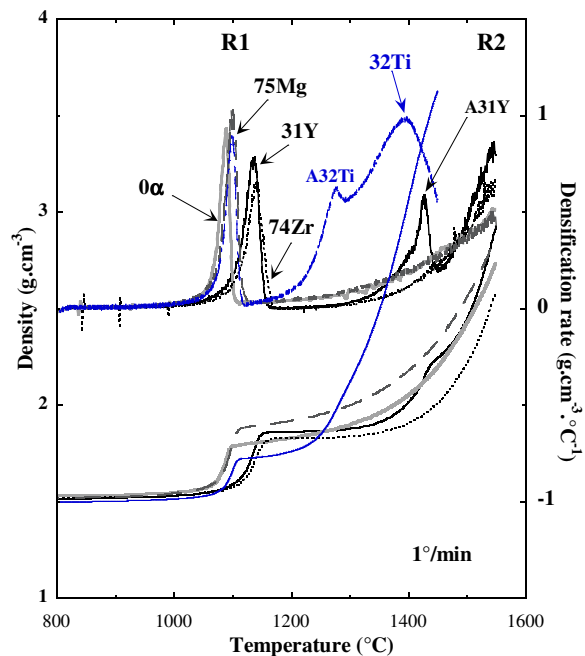


Fig. 5: densification curves of  $\gamma$  alumina compacts (250MPa CIP) doped with Mg (75Mg, 7500ppm Mg/Al), Zr (74Zr, 7400ppm Zr/Al), Y (31Y, 3100ppm Y/Al) and Ti (32Ti, 3200ppm Ti/Al).

Their solubility in  $\gamma$ -alumina is larger than the solubility in  $\alpha$ -alumina, so they may modify the parameters of phase transformation and may influence the GB diffusional properties and GB mobility during grain growth.

For doping contents less than the solubility limit in  $\alpha$ -phase, the doping element remain in solution in the growing  $\alpha$ -phase during the transformation and so would not strongly influence the first densification regime R1. For higher contents, the excess of the dopant has to be rejected to the surfaces and grain boundaries of  $\alpha$ -particles which grow at the expense of  $\gamma$ -grains. The resulting dopant surface and grain boundary segregation would increase the interface diffusion kinetics and consequently the densification rates. Moreover, the dopant may influence the rearrangement of the ions during the transformation: oxygen ions lattice changes from a cfc cubic packing to an hexagonal packing with a redistribution of aluminium cations in the octahedral sites involving short range diffusion of elements in the transformation interface.

While doping elements such as Mg, Y and Zr don't improve the  $\alpha$ -phase densification (R2), titanium doping greatly improves the densification of  $\alpha$ -alumina. These results are in agreement with creep experiments from which it has been deduced that yttrium and zirconium decrease GB diffusion [12] meanwhile Ti and Mg increase GB diffusion in comparison with undoped alumina [13]. It has been suggested that these differences in diffusional properties are correlated with differences in the ionicity of aluminium-oxygen bonds [14]. Titanium addition is known to strongly improve densification of  $\alpha$ -alumina. This increase in densification is interpreted as an increase in intergranular diffusion associated with an increase in GB mobility [15-17]. This accelerating densification in the  $\alpha$ -phase could be also explained by the fast decrease of internal porosity due to coarsening of elongated elementary bricks of porous colonies (Fig. 6) which have the same size than those in undoped alumina. Densification of such colonies leads to material with a final density close to the theoretical density but the grain sizes of the Ti-doped sintered samples remain very large.

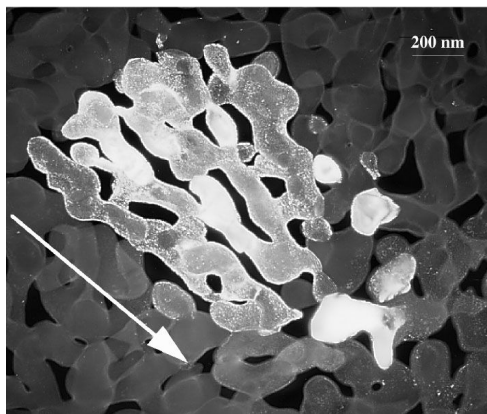


Fig. 6: TEM dark field image of  $^{32}\text{Ti}$  doped alumina sample showing elongated elementary bricks of porous monocrystalline colonies.

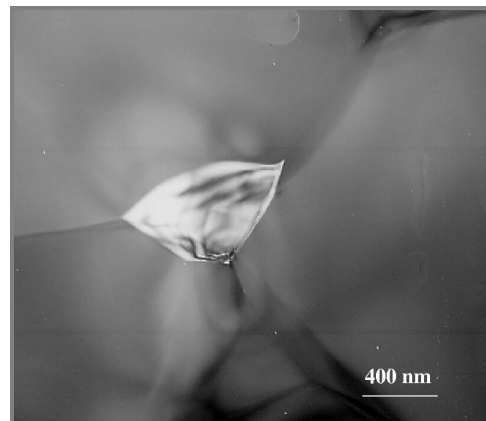


Fig. 7: TEM dark field image of  $\text{Al}_2\text{TiO}_5$  precipitates at triple junctions.

In addition to these two regimes, as already observed for Y-doped  $\alpha$ -alumina [18], a shoulder could be observed on the density curve with a corresponding abnormal densification rate peak (A) for Y and Ti-doping, its temperature depending on the doping level. This transient increase in densification rate is associated to a transition between a microstructure with only dopant intergranular segregation and a microstructure for which a precipitation of a second phase rich in doping element occurs at triple junctions (Fig. 7). As grain size increases the total area of interfaces decrease and the dopant concentration at GBs increases until the saturation of dopant at GBs over which precipitation occurs. During this transition, the increase in densification rate is attributed to

an acceleration of intergranular diffusivity that results from a supersaturation of dopant at GBs just before the precipitation. This transition implying a higher GB mobility allows to enhance the second densification regime, leading to final sintered density near to the theoretical one. Nevertheless, this transient increase in densification rate promotes concurrent grain growth, all the more it appears simultaneously with the maximum  $\alpha$ -phase densification rate (it's the case for 32Ti sample, Fig. 5). Although Mg and Zr-doping do not induce abnormal densification rate peak (A), XRD analyses performed on rapidly cooled samples from various temperatures of the second densification regime clearly show the presence of spinel phase or zirconia.

## Summary

The formation of stable  $\alpha$ -phase from  $\gamma$ -metastable phase occurs by a nucleation and controlled diffusion grain growth process during heating. Coupled mechanisms of transformation, rearrangement and coarsening from nucleation sites lead to the formation of monocrystalline porous colonies which consist of elementary bricks with similar crystallographic orientation. The influence of various doping elements on sintering behavior of the same  $\gamma$ -alumina has been analysed and showed that Mg, Y and Zr don't improve the densification in alpha phase, although titanium enhances this densification step by a fast decrease of internal porosity due to coarsening of elongated elementary bricks of porous colonies. To benefit from this effect and with the goal of producing sub-micrometric grain size dense ceramics using isothermal sintering, further work with controlled density of nucleation sites and co-doping to limit grain growth is planned.

## References

- [1] X.Z. Ding and X.H. Liu: *J. Mater. Res.* Vol. 13 (1998) p. 2556.
- [2] S.C. Liao, K.D. Pae, W.E. Mayo: *Mater. Sci. and Eng.* Vol. A204 (1995) p. 152.
- [3] F.W. Dynys and J.W. Halloran: *J. Amer. Ceram. Soc.* Vol. 65 (1982) p. 442.
- [4] G.L. Messing, M. Kumagai: *Am. Ceram. Soc. Bull.* Vol. 73 (1994) p. 88.
- [5] C. Legros, C. Carry and P. Bowen, H. Hofmann: *J. Eur. Ceram. Soc.* Vol. 19 (1999) p. 1967.
- [6] R.S. Mishra, C.E. Lesher, A.K. Mukherjee: *J. Am. Ceram. Soc.* Vol. 79 (1996) p. 2989.
- [7] L.A. Xue, I.W. Chen: *J. Mat. Sci. Lett.* Vol. 1 (1992) p. 443.
- [8] C. Carry, P. Bowen, F. Herbst, C. Legros: *Sintering Science and Technologies* (Ed. R.M. Germann, G.L. Messing, R.G. Cornwall, Penn. State Univ., PA USA 2000).
- [9] P. Bowen, O. Charvin and H. Hofmann, C. Carry, C. Herard: *Ceram. Trans.* Vol. 83 (1998) p. 211.
- [10] P. Bowen, M. Staiger and H. Hofmann, C. Carry: *Sintering Science and Technologies* (Ed. R.M. Germann, G.L. Messing, R.G. Cornwall, Penn. State Univ., PA USA 2000) p. 177.
- [11] P.I. Gouma, M.J. Mills: *J. Am. Ceram. Soc.* Vol. 84 [3] (2001) p. 619.
- [12] S. Lartigue-Korinek, C. Carry et L. Priester: *J. Eur. Ceram. Soc.* Vol. 22 (2002) p. 1525.
- [13] H. Yoshida, Y. Ikuhara and T. Sakuma: *Acta Mater.*, in press.
- [14] H. Yoshida, T. Yamamoto, Y. Ikuhara and T. Sakuma: *Phil. Mag. A* Vol. 82 (2002) p. 511.
- [15] Y.M. Kim, S.H. Song and D.Y. Kim: *J. Am. Ceram. Soc.* Vol. 83 (2000) p. 2809.
- [16] M. Kitayama, J.D. Powers, L. Kulinski and A.M. Glaeser: *Microstructures 96*, (Ed. Edited by A.P. Tomsia and A.M. Glaeser. Plenum Press, Berkeley, CA USA 1998).
- [17] J.D. Powers and A.M. Glaeser: *Ceram. Eng. Sci. Proc.* Vol. 18 [4] (1997) p. 617.
- [18] E. Sato and C. Carry: *J. Am. Ceram. Soc.* Vol. 79 (1996) p. 2156.

## **Diffusion in Materials - DIMAT2004**

10.4028/www.scientific.net/DDF.237-240

## **Phase Transformation and Densification of Nanostructured Alumina. Effect of Seeding and Doping**

10.4028/www.scientific.net/DDF.237-240.665

### **DOI References**

[3] F.W. Dynys and J.W. Halloran: J. Amer. Ceram. Soc. Vol. 65 (1982) p. 442.

doi:10.1111/j.1151-2916.1982.tb10511.x

[6] R.S. Mishra, C.E. Lesher, A.K. Mukherjee: J. Am. Ceram. Soc. Vol. 79 (1996) p. 2989.

doi:10.4028/www.scientific.net/MSF.225-227.617

[14] H. Yoshida, T. Yamamoto, Y. Ikuhara and T. Sakuma: Phil. Mag. A Vol. 82 (2002) p. 511.

doi:10.1080/01418610208239613

[16] M. Kitayama, J.D. Powers, L. Kulinski and A.M. Glaeser: Microstructures 96, (Ed. Edited by .P. Tomsia and A.M. Glaeser. Plenum Press, Berkeley, CA USA 1998).

doi:10.1023/A:1008656302007

[16] M. Kitayama, J.D. Powers, L. Kulinski and A.M. Glaeser: Microstructures 96, (Ed. Edited by A.P. Tomsia and A.M. Glaeser. Plenum Press, Berkeley, CA USA 1998).

doi:10.1023/A:1008656302007